

SIMULATION OF FLOW BOILING OF NANOFLUID IN TUBE BASED ON LATTICE BOLTZMANN MODEL

by

**Shouguang YAO^{a*}, Tao HUANG^a, Kai ZHAO^b,
Jianbang ZENG^c, and Shuhua WANG^a**

^a School of Energy and Power Engineering Zhenjiang,
Jiangsu University of Science and Technology, Jiangsu, China

^b China International Marine Containers (Group) Co., Ltd., Nantong, Jiangsu, China

^c Guangzhou Institute of Energy Conversion, Chinese Academy of Science Guangzhou,
Guangdong, China

Original scientific paper

<https://doi.org/10.2298/TSCI160817006Y>

In this study, a lattice Boltzmann model of bubble flow boiling in a tube is established. The bubble growth, integration, and departure of 3% Al₂O₃-water nanofluid in the process of flow boiling are selected to simulate. The effects of different bubble distances and lateral accelerations a on the bubble growth process and the effect of heat transfer are investigated. Results showed that with an increase in the bubble distance, the bubble coalescence and the effect of heat transfer become gradual. With an increase in lateral acceleration a , the bubble growth is different. When $a = 0.5e-7$ and $a = 0.5e-6$, the bubble growth includes the process of bubble growth, coalescence, detachment, and fusion with the top bubble and when $a = 0.5e-5$ and $a = 0.5e-4$, the bubbles only experience growth and fusion, and the bubbles do not merge with the top bubble directly to the right movement because the lateral acceleration is too large, resulting in the enhanced effect of heat transfer in the tube.

Key words: nanofluids, tube, lattice Boltzmann method, flow boiling

Introduction

Micro-channel boiling phenomenon has been widely used in the production and life of the society in recent years. For more than half a century, although people have been exploring the mechanism of boiling heat transfer and revealing the basic law of the boiling heat transfer, many unknown phenomena and mechanisms remain to be further explored. The study of the boiling heat transfer through the behavior characteristics of bubbles, as well as the bubble nucleation, growth, and detachment, in the channel is important to the heat dissipation in heat exchange equipment. Therefore, understanding the mechanism of bubble formation, growth, and detachment is the key to realize and optimize the boiling heat transfer process [1]. In recent years, a large number of single-bubble growth models have been reported in the process of nuclear boiling, and numerous theoretical results have been obtained for the bubble dynamics in pool boiling and large-distance flow boiling. Chatterjee and Chakraborty [2] formulated an enthalpy source-based model, which was based on a classical lattice Boltzmann scheme for describing internal energy evolution with a fixed-grid enthalpy-based formulation for the numerical simulation of the conduction-dominated phase change processes of single-compo-

* Corresponding author, e-mail: zjyaosg@126.com

ment systems. They used a single-particle density distribution function for calculating the thermal variable. Predictions from the model agreed excellently with the results obtained from established analytical/numerical models. Mukherjee and Kandlikar [3] used level set method to study the effect of micro-channel bubble growth on heat transfer and flow growth. The bubble growth rate increased with an increase in heat but decreased with an increase in the Reynolds number. The effect of gravity on the bubble growth rate was insignificant, and the numerical simulation results agreed with the results of the experimental observations.

Lattice Boltzmann method (LBM) has been developed in recent years. This method has the characteristics of microscopic particles, which can conveniently describe the interaction among phases and clearly capture the gas/liquid interface. Three main models exist in the field of multiphase flow in LBM, namely, the coloring model proposed by Gunstensen and Rothman *et al.* [4] in 1991, the pseudo potential model proposed by Shan and Gary [5], and the free-energy model proposed by Swift *et al.* [6]. In this study, based on the nanoparticle model proposed by Li [7] and combined with the pseudo potential model of Zeng [8], a multiphase composite LBM model that can describe the flow boiling of nanofluid was constructed. The bubble growth, jump off, and bubble dynamics in the boiling process of super-heated nanofluid were studied. The temperature field around the bubble was obtained, and the effect of heat transfer on the flow boiling of nanofluid was analyzed.

Nanofluid lattice Boltzmann composite model

Single component multiphase lattice Boltzmann evolution equation

The single component multiphase lattice Boltzmann evolution equation is [9]:

$$f_i(x + e_i \Delta t, t + \Delta t) - f_i(x, t) = -\frac{f_i(x, t) - f_i^{\text{eq}}(x, t)}{\tau} + \Delta f_i(x, t) \quad (1)$$

where τ is the non-dimensional relaxation time, which is related to the viscosity, ν , of nanoparticles [10], and $\nu = (2\tau - 1)c\Delta x/6$, $c = \Delta x/\Delta t$ – the particle migration rate, Δx – the lattice length, Δt – the discrete time step, $\Delta f_i(x, t)$ – the volume force term, $f_i(x, t)$ – the t time and x position out of the particle distribution function, $f_i^{\text{eq}}(x, t)$ – the corresponding equilibrium distribution function, and in D2Q9 model, the equilibrium distribution function is [10]:

$$f_i^{\text{eq}}(x, t) = \omega_i \rho(x, t) \left[\frac{1 + (e_i u)}{c_s^2} + \frac{(e_i u)^2}{2c_s^4} - \frac{u^2}{2c_s^2} \right] \quad (2)$$

where $\omega_0 = 4/9$, $\omega_i = 1/9$, $i = 1, \dots, 4$, $\omega_i = 1/36$, $i = 5, \dots, 8$, c_s is sound speed, then the macroscopic density and velocity are:

$$\rho(x, t) = \sum_{i=0}^8 f_i(x, t) = \sum_{i=0}^8 f_i^{\text{eq}}(x, t) \quad (3)$$

$$u(x, t) = \frac{\sum_{i=0}^8 e_i f_i(x, t)}{\rho(x, t)} \quad (4)$$

Because the interaction force between particles is introduced into the lattice Boltzmann model, it will affect the stability of the model, so this paper chooses the exact difference method proposed by Kupershtokh [11] to calculate the volume force, expressions are:

$$\Delta f_i(x, t) = f_i^{\text{eq}}[\rho(x, t), u(x, t) + \Delta u(x, t)] - f_i^{\text{eq}}[\rho(x, t), u(x, t)] \quad (5)$$

Speed change $\Delta u(x, t)$ is :

$$\Delta u(x, t) = \frac{\Delta M}{\rho(x, t)} = \frac{F_T(x, t)\Delta t}{\rho(x, t)} \quad (6)$$

where ΔM is the momentum change in each time step, $F_T(x, t)$ is interaction force between particles in a fluid and $F_1(x, t)$ is the adsorption force between fluid and wall $F_2(x, t)$, and external force $F_3(x, t)$, such as gravity. Then:

$$F_T(x, t) = F_1(x, t) + F_2(x, t) + F_3(x, t) \quad (7)$$

In order to separate the two phases, the interaction force of the different meeting needs to be considered, in this paper, according to the processing method of Yang and Tao [12], the state equation is obtained directly:

$$F_1(x, t) = -\nabla U(x, t), \quad \{U(x, t) = p[\rho(x, t), T(x, t)] - \rho(x, t)RT_0\} \quad (8)$$

where T_0 is related to the lattice model, in D2Q9 model, $T_0 = 1/3$, R – the universal gas constant, p – the gas state equation, $\varphi(x, t)$ – the interaction potential between particles, and $\varphi^2(x, t) = |U(x, t)|$, then:

$$F_1(x, t) = 2\varphi(x, t)\nabla\varphi(x, t) \quad (9)$$

To adsorption force between fluid and wall $F_2(x, t)$, in this paper, we refer to the processing methods in [13], the expressions are:

$$F_2(x, t) = -G_w\rho(x, t)\sum_i s(x + e_i, t)e_i \quad (10)$$

where $x + e_i$ is on a solid node, then $s(x + e_i, t) = 1.0$, unless $s(x + e_i, t) = 0$, in which G_w is strength of interaction between fluid and solid wall. External force $F_3(x, t)$ can express:

$$F_3(x, t) = \rho(x, t)g \quad (11)$$

where g is the acceleration of fluid motion, the expression of the true velocity of the fluid is:

$$\rho(x, t)u(x, t) = \frac{F_T(x, t)\Delta t}{2} + \sum_{i=0}^8 e_i f_i(x, t) \quad (12)$$

According to [8], compared to the model proposed by Zhang and Chen [14], the model of Kupershtokh [11] changed the way of finding the volume force, the solution of the model is more simple, and because of the correction of speed, the pseudo speed is reduced, and the stability of the model is improved, the application range of the model is more extensive.

Energy equation

The investigation of non-homogeneous boiling phenomena requires considering the energy transfer process. In the lattice Boltzmann model, there are two main ways to deal with the energy equation: by introducing the mesoscopic energy conservation equation, use the finite difference method or the finite volume method to solve the temperature field; this kind of thinking is visually appealing, but at present, the model still has the defects of poor computational stability [14] and Couple the energy equation and momentum equation to solve [15], by introducing the temperature distribution function, the evolution equation is:

$$g_i(x + e_i \Delta t, t + \Delta t) - g_i(x, t) = -\frac{g_i(x, t) - g_i^{\text{eq}}(x, t)}{\tau_2} - \omega_i \Delta t q \quad (13)$$

where q is heat flux density in time step t , and the distribution function of the temperature equilibrium state is:

$$g_i^{\text{eq}}(x, t) = \omega_i \left[T + \frac{T(e_i u)}{c_s^2} - \frac{\tilde{D}_T(e_i \nabla T)}{c_s^2} \right] \quad (14)$$

where $\tilde{D}_T = D_T + (2\tau_2 - 1)c\Delta x/6$, D_T is temperature diffusion coefficient, and the temperature is:

$$T(x, t) = \sum_{i=0}^8 g_i(x, t) \quad (15)$$

Using the Chapman-Enskog expansion technique, combined with eqs. (3) and (15), ignoring the higher order terms, we can find eqs. (1) and (13) the corresponding macroscopic momentum and energy equations respectively:

$$\frac{\partial \rho}{\partial t} + \nabla(\rho u) = 0, \quad \frac{\partial(\rho u)}{\partial t} + \nabla(\rho u u) = -\nabla(c_s^2 \rho) + \nu \nabla^2 u \quad (16a)$$

$$\frac{\partial T}{\partial t} + \nabla(Tu) = \nabla(D_T \nabla T) - q \quad (16b)$$

Heat flux density

The entropy equilibrium equation with viscous dissipation neglected is expressed:

$$\rho T \frac{ds}{dt} = \nabla(\lambda \nabla T) \quad (17)$$

where s is entropy, and λ is thermal conductivity. According to the basic equation of thermodynamics:

$$T ds = c_v dT + T \left(\frac{\partial p}{\partial T} \right)_v dv \quad (18)$$

where c_v is constant volume specific heat. If the system is fixed, it can be written:

$$T ds = c_v dT - T \left(\frac{\partial p}{\partial T} \right)_\rho \frac{d\rho}{\rho^2} \quad (19)$$

Simultaneous (19) and (16):

$$\rho c_v \frac{dT}{dt} = \nabla(\lambda \nabla T) + \rho T \left(\frac{\partial p}{\partial T} \right)_\rho \frac{d\rho}{\rho^2} \quad (20)$$

Compared eqs. (16b) and (20), $D_T = \lambda/(\rho c_v)$, then the heat flux density is:

$$q = -T \left(\frac{\partial p}{\partial T} \right)_\rho \frac{d\rho}{\rho^2 c_v} \quad (21)$$

Dimensional transformation

When we use of LBM simulation, it is necessary to carry out the dimensional transformation, assuming that the length L' , time T' , and quality G' are grid units, L , T , and G are the length, time, and quality of the actual physical unit. If the tube diameter is, D , the kinematic viscosity is ν , fluid density is ρ . They are converted to [16]:

$$D = D'L, \quad \nu = \nu' \frac{L^2}{T}, \quad \rho = \rho' \frac{G}{L^3} \quad (22)$$

where D' is the lattice unit diameter, ν' is the lattice kinematic viscosity, ρ' is the lattice fluid density. It can be concluded that the actual physical quantity are:

$$L = \frac{D}{D'}, \quad T = \frac{\nu'}{\nu} \left(\frac{D}{D'} \right)^2, \quad G = \frac{\rho}{\rho'} \left(\frac{D}{D'} \right)^3 \quad (23)$$

Physical parameters

In this paper, the research object is 3% Al_2O_3 - H_2O nanofluid, and tab. 1 is the physical properties of Al_2O_3 nanoparticles.

The physical parameters of the nanofluids are calculated:

The capacity of nanofluids is expressed [17]:

$$\rho_{\text{nf}} c_{p_{\text{nf}}} = (1 - \phi) \rho_f c_{p_f} + \phi \rho_p c_{p_p} \quad (24)$$

where c_{p_f} and c_{p_p} are the capacities of base fluids and nanoparticle. The ϕ is the volume fraction of nanofluids, ρ_f – the destiny of base fluids, ρ_p – the destiny of nanoparticle.

The viscosity of nanofluids is expressed [18]:

$$\mu_{\text{nf}} = \mu_f (1 + 39.11\phi + 533.9\phi^2) \quad (25)$$

where μ_f is the viscosity of base fluids.

The coefficient of thermal conductivity of nanofluids is expressed [19]:

$$\frac{k_{\text{nf}}}{k_f} = \frac{k_p + 2k_f - 2\phi(k_f - k_p)}{k_p + 2k_f + \phi(k_f - k_p)} \quad (26)$$

where k_p and k_f are the thermal conductivity of nanoparticle and base fluids.

The thermal diffusion coefficient of nanofluids is expressed [19]:

$$\alpha_{\text{nf}} = \frac{k_{\text{nf}}}{(\rho c_p)_{\text{nf}}} \quad (27)$$

Simulation results and analysis

Initial state and boundary conditions

When the simulation starts, a constant acceleration a is given in the horizontal direction, and the gravity acceleration in the vertical direction is g , as shown in fig. 1. The calculation area is 300×150 rectangular, $\Delta x = \Delta t$, $c = 1.0$, and $c_s = c/3^{1/2} = 1.0/3^{1/2}$. The upper and lower

Table 1. Physical properties

Physical properties	Water	Nanoparticle (Al_2O_3)
ρ [kgm^{-3}]	997.1	3970
c_p [$\text{Jkg}^{-1}\text{K}^{-1}$]	4174	765
ν [m^2s^{-1}]	$8.05\text{e}-7$	–
k [$\text{Wm}^{-1}\text{K}^{-1}$]	0.618	25
$\sigma \cdot 10^{-3}$ [Nm^{-1}]	69	–

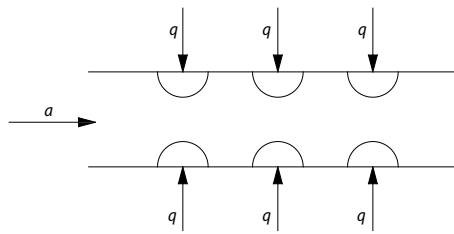


Figure 1. Physical model

lower boundaries of the given vaporization core. Thus, the nodes in the center of the upper and lower boundaries are the first to undergo phase change. The bubble is constantly becoming larger because of the continuous introduction of heat flux at the vaporization core before the bubble separates from the wall.

Bubble growth process

The initial moment of calculation does not require a given bubble nuclear radius because the heat flux is large enough, and the fluid that surrounds the nuclear core can be vaporized rapidly. If the surface tension is large enough at this time, the core will form a gas core. With the further introduction of heat flux, the air core gradually grows into a bubble. When the bubble diameter is raised to the departure diameter, the bubble will separate from the bottom wall. Owing to the effect of the lateral acceleration of a , the bubble growth is also affected by the horizontal direction force. Given that the bubble is affected by the transverse force, the bubble will fuse during the growth process. Taking two bubbles as an example, in this effect, the initial temperature remains $0.86T_c$, the gravity is constant $g = 1.2 \cdot 10^{-5}$, $\Delta x = \Delta t$, $c = 1.0$, and $c_s = c/3^{1/2} = 1.0/3^{1/2}$. The upper and lower walls of the pipe are provided with two vaporization cores, the distance is 60 units, and the lateral acceleration is $a = 0.5e - 5$. The program converges when the program runs to $10e-6$. The processes of bubble growth and fusion in the tube are simulated in fig. 2. A distinct difference exists between the upper wall and the lower growth of the bubble, and the main difference is that the low wall bubbles have a clear upward growth trend, mainly because the bottom wall bubbles are forced by the upward buoyancy. When the bubble diameter is raised to the departure diameter, the bubble will be separated from the bottom wall. The upper wall bubbles are also affected by vertical upward buoyancy. Therefore, the downward trend is not obvious, and the bubble will fuse with the bottom bubbles as soon as they separate from the bottom wall.



Figure 2. Two bubbles growth process (for color image see journal web site)

Influence of bubble growth process on the heat transfer in tube

The initial temperature remains $0.86T_c$, the gravity is constant $g = 1.2 \cdot 10^{-5}$, $\Delta x = \Delta t$, $c = 1.0$, and $c_s = c/3^{1/2} = 1.0/3^{1/2}$ to study the influence of the bubble growth process on the heat transfer in tube. The upper and lower walls of the pipe are provided with three vaporization

boundaries are used to bounce back boundary, and the density and temperature correspond to the physical amount of saturation pressure. The heat flux is introduced by the upper and lower boundaries of the given vaporization core, and the periodic boundary is adopted. The initial temperature is $0.86T_c$, and the gravity is constant $g = 1.2 \cdot 10^{-5}$. Assuming that the system is isobaric, the calculation of fluid within the region is in the saturated state. The heat flux is introduced by the upper and

cores, the distance is 60 units, and the lateral acceleration is $a = 0.5e-6$. The distribution of temperature field at different times is illustrated in fig. 3.

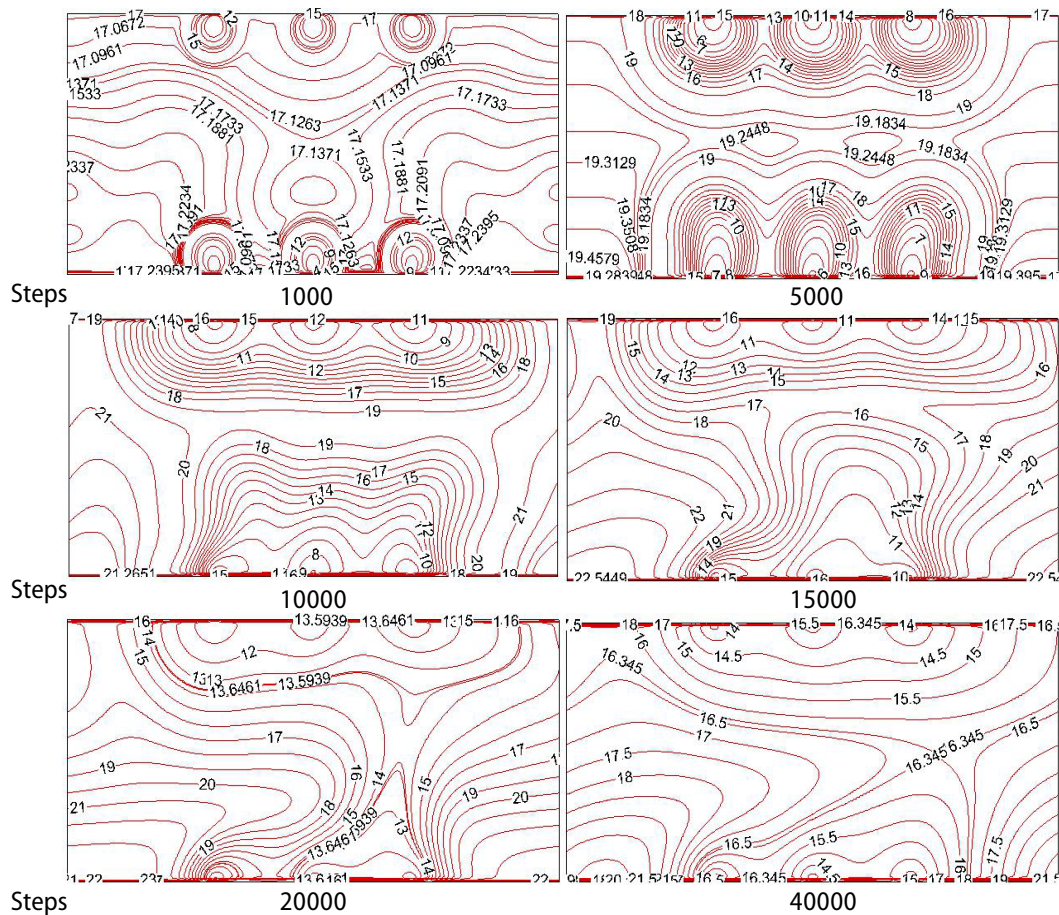


Figure 3. Distribution of temperature field

Influence of bubble distance

The initial temperature remains $0.86T_c$ while other parameters are unchanged and the gravity is constant $g = 1.2 \cdot 10^{-5}$ to study the influence of bubble distance on the bubble growth. The number of bubbles is increased to 3, and the distances are 20, 30, 50, 60, and 70 units, as shown in fig. 4.

Figure 4 presents that when the bubble distance is 20 units, the bubbles begin to fuse in the 3000 steps and separate and fuse with the top bubbles in the 15000th step. When the bubble distance is 30 units, the bubbles start to fuse in the 5000th step and separate in the 15000th step. When the bubble distances are 50 and 60 units, the bubbles all fuse in the 15000th step and separate in the 30000th step. When the bubble distance is 70 units, the bubbles do not fuse until the 20000th step and separate in the 45000th step. With an increase in the distance among bubbles, the initial fusion time is also increased. When the bubble distance is 60 units, the bubble evolution process is relatively smooth, which has an obvious effect on the heat transfer in the tube.

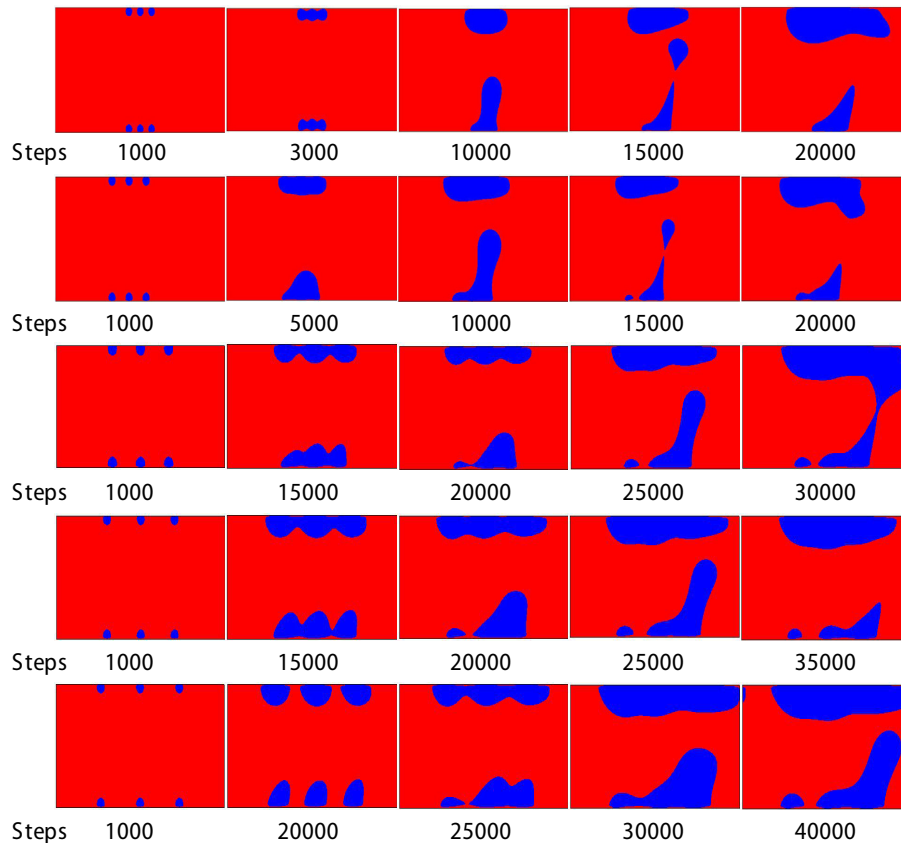


Figure 4. The growth process of bubbles in different distances
(for color image see journal web site)

Influence of lateral acceleration a on the bubble growth process in the tube

The initial temperature remains $0.86T_c$ while other parameters are unchanged and the gravity is constant $g = 1.2 \cdot 10^{-5}$ to study the influence of lateral acceleration, a , on the bubble growth. The number of bubbles is 3, the distance is 60 units, and the lateral accelerations, a , are $a = 0.5e-7$, $a = 0.5e-6$, $a = 0.5e-5$, and $a = 0.5e-4$. The growth process of bubbles in different lateral accelerations, a , is illustrated in fig. 5.

When $a = 0.5e-7$, the growth process of the bubbles is almost unaffected by the lateral acceleration, a . The growth process presents a vertical rise, but the growth process is still divided into growing up, merging together, and separating. When $a = 0.5e-6$, the lateral acceleration, a , has an inconsiderable influence on the bubble growth process, that is, the bubbles move to the right side during the rising process. Accordingly, the growth process of the bubbles is oblique and has the processes of merging together and separating. When $a = 0.5e-5$ and $a = 0.5e-4$, the lateral acceleration, a , has an obvious effect on the bubble growth process. When a is large, the bubbles cannot fuse with the top wall bubbles and move to right directly after separating from the bottom wall. With an increase in the lateral acceleration, a , the heat transfer effect is strengthened.

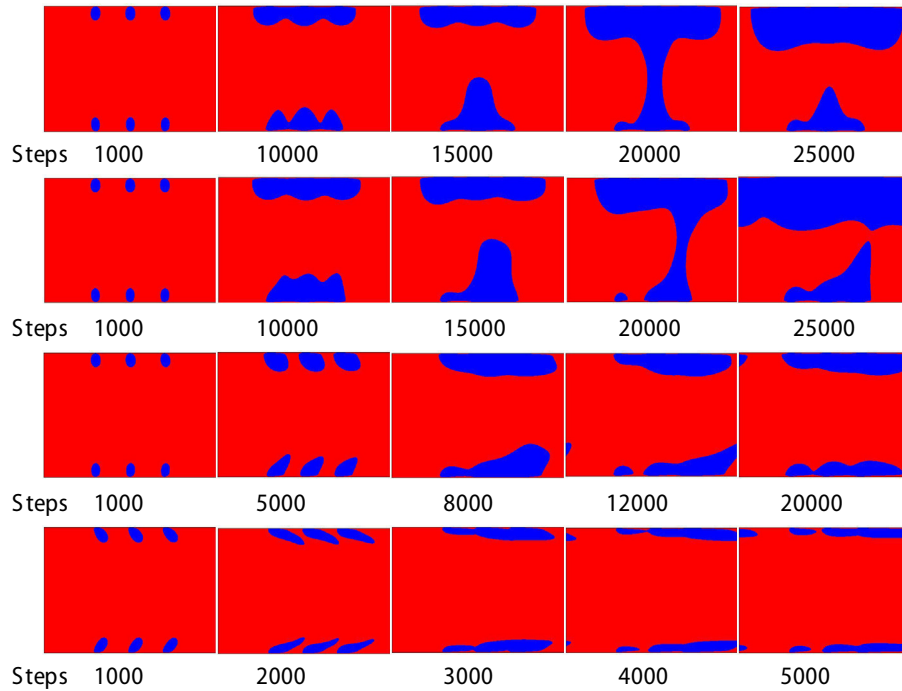


Figure 5. Bubble growth process in different lateral acceleration a
 (for color image see journal web site)

Conclusions

In this study, a lattice Boltzmann model of nanofluid flow boiling in a tube is established. The effect of different bubble distances and lateral accelerations, a , on the bubble growth process and the effect of heat transfer are simulated. The conclusions are as follows.

- With an increase in the bubble distance, the velocity of bubble fusion becomes slower, the frequency of the bubble separation decreases, and the heat reduction of the unit time from the bubble decreases, which lead to a decreased heat transfer effect.
- With an increase in the lateral acceleration, a , the bubble growth experiences different processes. When a is small, the bubble growth increases, fuses together, separates from the bottom wall, and fuses with the top bubbles. When a is large, the bubbles only experience growth and fusion. Given that the lateral acceleration is too large, the bubble departure frequency increases. The heat reduction of the unit time from the bubble also increases, which strengthens the heat transfer effect in the tube.

Acknowledgement

This work was supported by National Natural Science Foundation of China under Grant No. 51176069.

Nomenclature

a	– acceleration, [ms^{-2}]	g	– gravitational acceleration, [ms^{-2}]
c	– sound velocity,	k	– thermal conductivity
G_w	– strength of interaction between fluid and solid wall	q	– heat flux density
		T	– dimensionless temperature, [–]

t – total step
 Δt – time step
 u, v, w – velocities, [ms⁻¹]
 x, y, z – coordinates, [m]
 Δx – grid step

Greek symbols

α – thermal diffusivity, [m²s⁻¹]
 γ – density ratio of gas and liquid
 μ – dynamic viscosity, [kgm⁻¹s⁻¹]
 ν – kinematic viscosity, [m²s⁻¹]

ρ – density, [kgm⁻³]
 σ – different components
 ϕ – nanoparticles volume fraction
 Θ – phase change rates

Subscript

$b \rightarrow r$ – liquid phase to gas phase
 f – fluid
 nf – nanofluid
 $r \rightarrow b$ – gas phase to liquid phase

Reference

- [1] Xiao, B. Q., et al., Mathematical Analysis of Pool Boiling Heat Transfer, *Journal of Physics*, 58 (2009), Apr., pp. 25-35
- [2] Chatterjee, D., Chakraborty, S., An Enthalpy-Source Based Lattice Boltzmann Model for Conduction Dominated Phase Change of Pure Substances, *Int. J. Thermal Science*, 47 (2008), 5, pp. 552-559
- [3] Mukherjee, A. S., Kandlikar, G., Numerical Simulation of Growth of a Vapor Bubble Duringflow Boiling of Water in A Microchannel, *Microfluid Nanofluid*, 1 (2005), 2, pp. 137-145
- [4] Gunstensen, A. K., Rothman, D. H., A Galilean Invariant Immiscible Lattice Gas, *Physica*, 47 (1991), 2, pp. 53-63
- [5] Shan, X. W., Gary, D., Multicomponent Lattice Boltzmann Model with Interparticle Interaction, *Journal of Statistical Physics*, 81 (1995), 2, pp. 379-393
- [6] Swift, M., et al., Lattice Boltzmann Simulations of Liquid-Gas and Binary Fluid Systems, *Phys. Rev. E*, 54 (1996), 5, 5041
- [7] Li. R. J., Numerical Simulation of Evaporation Behavior and Solute Deposit of a Sessile Droplet on Substrates, Academic Resource Repository, Kochi University of Technology, Kami, Japan, 2012
- [8] Zeng, J. B., et al., Lattice Boltzmann Method Simulation of Bubble Growth in Pool Boiling, *Journal of Physics*, 60 (2011), 066401
- [9] Zeng, J. B., et al., Simulation of Boiling Process with Lattice Boltzmann Method, *Journal of Xi'an Jiaotong University*, 43 (2009), 7, pp. 25-29
- [10] Guo, Z. L, Zheng, C. G., *Theory and Application of Lattice Boltzmann Method*, Science Press, Beijing, 2009
- [11] Kupershtokh, A. L., New Method of Incorporating a Body Force Term into the Lattice Boltzmann Equation, *Proceedings*, 5th International EHD Workshop Poitiers-France, 2004, pp. 241-246
- [12] Yang, S. M., Tao, W. Q., *Heat Transfer Theory*, Higher Education Press, Beijing, 1998
- [13] Martys, N. S., Chen, H., Simulation of Multicomponent Fluids in Complex Three-Dimensional Geometries by the Lattice Boltzmann Method, *Physical Review: E*, 53 (1996), 1, pp. 743-750
- [14] Zhang, R. Y., Chen, H. D., Lattice Boltzmann Method for Simulations of Liquid-Vapor Thermal Flows, *Physical Review E*, 67 (2003), June, 066711
- [15] Hazi, G., Markus, A., On the Bubble Departure Diameter and Release Frequency Based on Numerical Simulation Results, *Int. J. of Heat and Mass Transfer*, 52 (2009), 5-6, pp. 1472-1480
- [16] Yan, W. W., *Lattice Boltzmann Simulation of Cell Adhesion in Microcirculation*, The Hong Kong Polytechnic University, Hong Kong, China, 2011
- [17] Gherasim, I., et al., Experimental Investigation of Nanofluids in Confined Laminar Radial Flows, *International Journal of Thermal Science*, 48 (2009), 8, pp. 1486-1493
- [18] Nguyen, C. T., Desgranges, F., Temperature and Particle-Size Dependent Viscosity Date for Water-Based Nanofluids-Hysteresis Phenomenon, *International Journal of Heat and Fluid Flow*, 28 (2007), 6, pp. 1492-1506
- [19] Kuppusamy, N. R., et al., Numerical Investigation of Trapezoidal Grooved Microchannel Heat Sink Using Nanofluids, *Thermochimica Acta*, 573 (2013), Dec., pp. 39-56